Three-Dimensional Flow in Rotating Rocket Motor Nozzles

Jeffrey J. Brown*
Boeing Commercial Airplane Company, Seattle, Washington
and
Joe D. Hoffman†
Purdue University, West Lafayette, Indiana

A procedure used to calculate the effects of rocket motor rotation on the subsonic/transonic flowfield in axisymmetric rocket motor nozzles is presented. The governing equations for the unsteady three-dimensional flow of an ideal, inviscid fluid in thermodynamic equilibrium are derived in a noninertial reference frame. The governing equations are integrated numerically using MacCormack's explicit finite difference method. The boundary conditions are applied using Kentzer's method. The present technique is used to provide an accurate, steady, supersonic, initial-value surface for an existing method-of-characteristics analysis for steady three-dimensional supersonic flow. The steady supersonic initial-value surface is obtained as the asymptotic solution for large time of the unsteady subsonic/transonic flow analysis. This procedure can also be used to calculate the effects of inlet flow misalignment on the subsonic/transonic flowfield in nozzles.

Nomenclature

M	= Mach number
p	= static pressure
r,θ,z	= coordinates
$\bar{R}$, $\bar{r}$	= position vectors, inertial and noninertial reference frames, respectively
t	= time
v	= velocity component
$\bar{V}$	= velocity vector
$\bar{X}$	= body force vector
ρ	= density
$\bar{\omega}$	= angular acceleration vector

Subscripts

M	= relative to the missile
N	= relative to the nozzle
r,θ,z	= components
XYZ, xyz	= inertial and noninertial reference frames, respectively

Introduction

THE objective of this investigation[1,2] was to develop an analysis and a computer program to predict the unsteady three-dimensional subsonic/transonic flowfields that occur in the inlets and throats of axisymmetric rocket motor nozzles, including the effects of rotation and inlet flow misalignment. The results of the present method can be used to provide an accurate steady supersonic initial-value surface (IVS) for an existing method-of-characteristics (MOC) analysis of the steady supersonic flowfield in the diverging portion of the nozzle.[3]

One technique for generating the maneuvering torque for a fast response system is to rotate the supersonic portion of the propulsive nozzle to create a thrust misalignment and a corresponding turning torque. In the analysis of such a system, two questions arise: 1) how much missile turning torque is generated by a specified amount of nozzle rotation, and 2) what torque is required of the nozzle actuation system to rotate the nozzle to the desired position? The present investigation is directed toward the calculation of these effects.

A common problem arising in the design of rocket motor nozzles is the effect of inlet flow misalignment on the subsonic/transonic flowfield in the nozzle. Inlet flow misalignment results in thrust vector misalignment. Inlet flow misalignment may be intentional (i.e., for thrust vector control) or unintentional (i.e., manufacturing or assembly tolerance buildup). The present investigation is also directed toward the calculation of this effect.

The computer code developed in the present investigation is an extension of the VNAP code developed by Cline.[4]

Background

Effect of Rotation

Figure 1 illustrates a missile rotating with the angular velocity $\bar{\omega}_M$ and angular acceleration $\bar{\alpha}_M$ with respect to the inertial reference frame XYZ fixed on Earth, and a nozzle rotating with the angular velocity $\bar{\omega}_N$ and angular acceleration $\bar{\alpha}_N$ with respect to the missile. The angular velocity of the nozzle with respect to the inertial reference frame is $\bar{\omega}=\bar{\omega}_M+\bar{\omega}_N$, and the angular acceleration of the nozzle with respect to the inertial reference frame is $\bar{\alpha}=\bar{\alpha}_M+\bar{\alpha}_N$. The missile may also have linear velocity $\bar{V}_M$ and linear acceleration $\bar{a}_M$ with respect to the inertial reference frame XYZ.

Hoffman and Vadyak[3] developed an analysis and a computer program for calculating the steady three-dimensional flowfield in a rotating supersonic nozzle using an MOC formulation. Due to the assumption of steady flow, that analysis is applicable only in a quasisteady sense to the steady portion of a nozzle rotational movement. The program requires a supersonic IVS just downstream of the nozzle throat. When the missile and nozzle inlet are not rotating, several techniques exist for calculating the required IVS, see, for example, Kliegel and Levine.[5] The effects of rotation on the flow in the supersonic portion of the nozzle can then be calculated. Figure 2 presents some results obtained by Vadyak et al.[6] using the aforementioned program. The curve labeled "nozzle rotation only" was obtained for $\bar{\omega}_M=\bar{\alpha}_M=\bar{\alpha}_N=0$.

When the missile is also rotating, the Coriolis and centripetal accelerations also act on the flow inside the grain perforation and nozzle inlet, and consequently affect the supersonic IVS at the nozzle throat. The missile rotation rate and moment arm from the missile center of gravity to the nozzle exit may be significantly larger than the nozzle rotation rate

Presented as Paper 84-0260 at the AIAA 22nd Aerospace Sciences Meeting, Reno, NV, Jan. 9-12, 1984; submitted Sept. 11, 1984; revision submitted May 16, 1985.

*Senior Specialist Engineer, Propulsion Research Unit. Member AIAA.

†Professor of Mechanical Engineering, Thermal Sciences and Propulsion Center. Member AIAA.

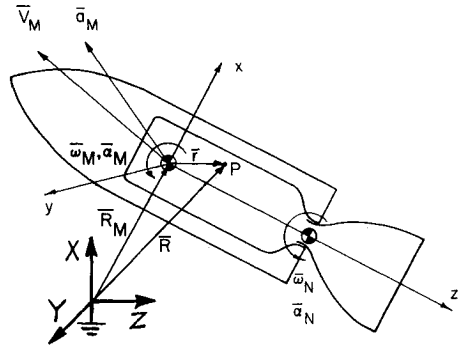

Fig. 1 Rotating missile and nozzle coordinate systems.

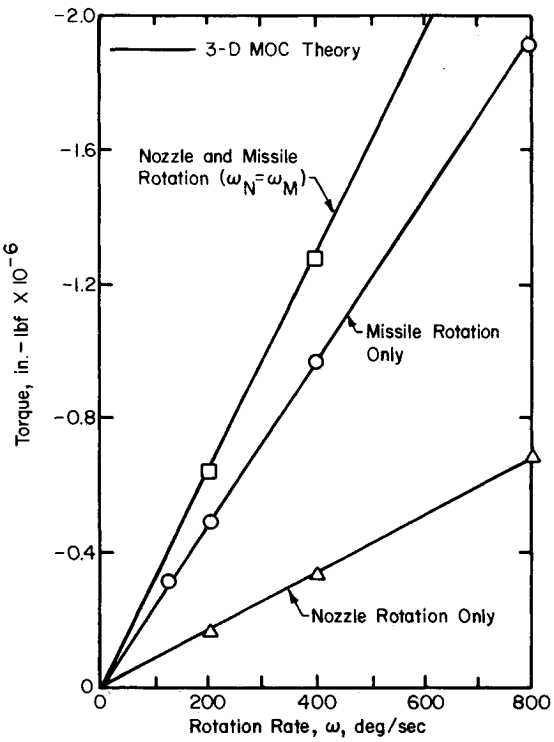

Fig. 2 Variation of nozzle torque with rotation rate.

and moment arm. Consequently, the effects of missile rotation on the flowfield in the grain perforation and nozzle inlet may be as significant as the effects in the supersonic portion of the nozzle. The present study addresses these effects.

Figure 2 also presents some results obtained by Vadyak et al.,[6] including the effects of missile rotation on the flowfield inside the supersonic portion of the nozzle, but neglecting the effects of missile rotation on the upstream flowfield and supersonic IVS. The curve labeled "missile rotation only" pertains to the case where the nozzle is not rotating with respect to the rotating missile. The curve labeled "combined nozzle and missile rotation" pertains to the case where the nozzle is rotating with respect to the rotating missile with $\bar{\omega}_N = \bar{\omega}_M$. From these results it is obvious that the effect of missile rotation, both alone and combined with nozzle rotation, significantly increases the torque on the nozzle. However, these results are uncertain due to the unknown effect of missile rotation on the upstream flowfield. In view of the large increase in torque when the missile is rotating, it is necessary to account for the effects of Coriolis and centripetal accelerations on the upstream flowfield so that a realistic supersonic IVS may be obtained for the supersonic flowfield analysis.

The analysis presented herein considers the effect of missile rotation on the nozzle subsonic/transonic flowfield as well as on the supersonic IVS discussed above. Several simplifications of the physics of the problem have been made. They are: 1) the fluid is an ideal gas in thermodynamic equilibrium, 2) the effect of rotation on the flowfield in the solid propellant grain is negligible, and 3) the subsonic/transonic portion of the nozzle is fixed to the missile and does not rotate with respect to the missile. Only the supersonic portion of the nozzle rotates with respect to the missile. The first assumption is adequate to test the concept. Furthermore, a real gas model could be added to the code as an enhancement. The addition of condensed phases would be a major effort. Clearly, the present model yields only qualitative results when condensed phases are present. In the solid propellant grain the fluid velocities are small, minimizing the effects of rotation on that flowfield.

The solution for a given combination of missile rotation and rotation of the supersonic nozzle is obtained in the following manner. The present unsteady method[2] is employed to march in time to yield a steady supersonic IVS for a given missile rotation rate. This is done to take advantage of the hyperbolic nature of the governing equations for unsteady subsonic/transonic flow. The steady supersonic IVS is obtained from the unsteady method developed herein as the asymptotic solution for large time. The steady MOC analysis[3] is then employed to calculate the steady supersonic nozzle flowfield under the combined effects of missile and nozzle rotation.

Effect of Inlet Flow Misalignment

Figure 3 illustrates a nozzle with a misaligned inlet flow. Hoffman and Maykut[7] presented an analysis of this situation when the flow misalignment occurred at the nozzle throat. In that case, the subsonic/transonic flowfield is axisymmetric. Only the supersonic flowfield is three-dimensional. Figure 4 presents some results for throat flow misalignment in conical nozzles. That figure presents side specific impulse as a function of nozzle length for conical nozzles having cone angles of 0, 5, 10, 15, 20, and 25 deg, for 1.0 deg of throat flow misalignment. The results show that the magnitude of the side force varies as the nozzle length increases, and even changes sign. Such results have a major impact on the design of thrust vector control systems.

The results obtained by Hoffman and Maykut[7] are limited to throat flow misalignment. When flow misalignment occurs at the subsonic nozzle inlet, the subsonic/transonic flowfield becomes three-dimensional. The present study also addresses this problem.

Gasdynamic Model

The major assumptions employed in the gasdynamic model are: 1) inviscid flow; 2) external forces due to noninertial effects only; 3) no heat transfer, external work, or mass diffusion; and 4) the fluid is a perfect gas. The governing equations consist of the continuity equation, component momentum equations, energy equation, and the thermal and caloric equations of state. The continuity and energy equations are applicable in any reference frame, where the fluid velocity is measured with respect to that reference frame. The component momentum equations, however, are applicable only in an inertial reference frame.

Figure 1 illustrates the physical arrangement. The Cartesian coordinate system XYZ is an inertial reference frame attached to Earth. The missile is located at the position $\bar{R}_M$ with respect to the inertial reference frame. Nozzle rotation relative to the missile is not considered in this analysis. The analysis including both missile and nozzle rotation is presented by Hoffman and Vadyak.[3] The Cartesian coordinate system xyz is a noninertial reference frame attached to the missile. The location of point P in the flowfield is denoted by $\bar{R}$ and $\bar{r}$ in the inertial and noninertial reference frames, respectively. The flowfield in the propulsive nozzle is obtained by solving for the flowfield relative to the noninertial reference frame. This

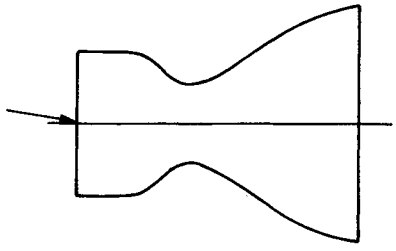

Fig. 3 Misaligned inlet flow.

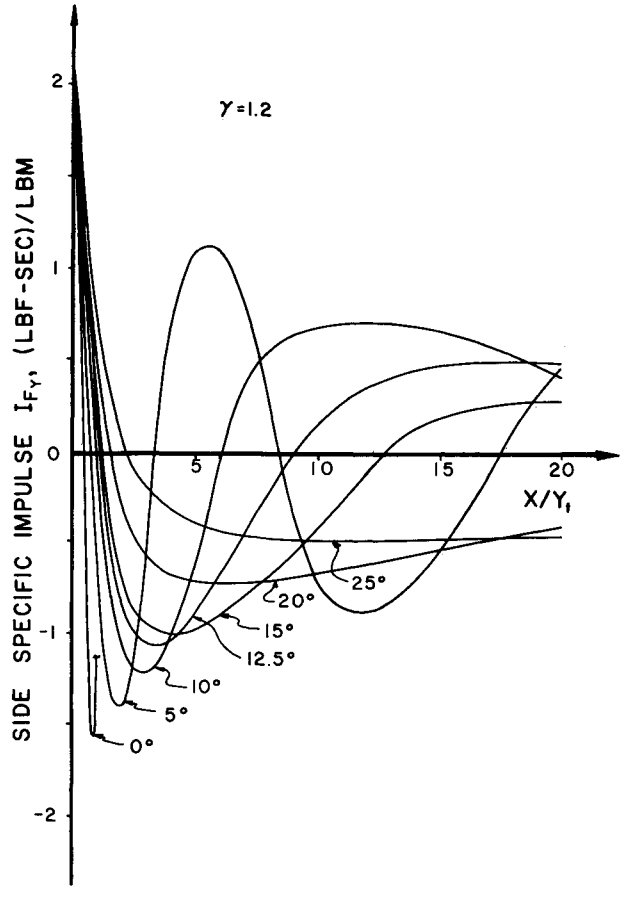

Fig. 4 Effect of cone angle on side specific impulse.

is accomplished by expressing the governing equations in the noninertial reference frame.

Expressing the continuity equation, the three-component momentum equations, and the energy equation in cylindrical coordinates in the noninertial reference frame yields (see Ref. 2):

$$\frac{\partial \rho}{\partial t}+v_r\frac{\partial \rho}{\partial r}+\frac{v_\theta}{r}\frac{\partial \rho}{\partial \theta}+v_z\frac{\partial \rho}{\partial z}+\rho\left(\frac{\partial v_r}{\partial r}+\frac{v_r}{r}+\frac{1}{r}\frac{\partial v_\theta}{\partial \theta}+\frac{\partial v_z}{\partial z}\right)=0 \quad (1)$$

$$\frac{\partial v_r}{\partial t}+v_r\frac{\partial v_r}{\partial r}+\frac{v_\theta}{r}\frac{\partial v_r}{\partial \theta}+v_z\frac{\partial v_r}{\partial z}-\frac{v_\theta^2}{r}+\frac{1}{\rho}\frac{\partial p}{\partial r}=X_r \quad (2)$$

$$\frac{\partial v_\theta}{\partial t}+v_r\frac{\partial v_\theta}{\partial r}+\frac{v_\theta}{r}\frac{\partial v_\theta}{\partial \theta}+v_z\frac{\partial v_\theta}{\partial z}+\frac{v_r v_\theta}{r}+\frac{1}{\rho r}\frac{\partial p}{\partial \theta}=X_\theta \quad (3)$$

$$\frac{\partial v_z}{\partial t}+v_r\frac{\partial v_z}{\partial r}+\frac{v_\theta}{r}\frac{\partial v_z}{\partial \theta}+v_z\frac{\partial v_z}{\partial z}+\frac{1}{\rho}\frac{\partial p}{\partial z}=X_z \quad (4)$$

$$\frac{\partial p}{\partial t}+v_r\frac{\partial p}{\partial r}+\frac{v_\theta}{r}\frac{\partial p}{\partial \theta}+v_z\frac{\partial p}{\partial z}-a^2\left(\frac{\partial \rho}{\partial t}+v_r\frac{\partial \rho}{\partial r}+\frac{v_\theta}{r}\frac{\partial \rho}{\partial \theta}+v_z\frac{\partial \rho}{\partial z}\right)=0 \quad (5)$$

where ρ is the density; p the pressure; a the speed of sound; v_r, v_θ, and v_z the velocity components; and X_r, X_θ, and X_z the components of the external force $\bar{X}$ in cylindrical coordinates r, θ, and z, respectively; t the time, and $\bar{X}$ is given by

$$\bar{X}=-[\bar{a}_M+2\bar{\omega}_M\times\bar{V}_{xyz}+\bar{\omega}_M\times(\bar{\omega}_M\times\bar{r})+\bar{\alpha}_M\times\bar{r}\,] \quad (6)$$

Unit Processes

Computation of the flowfield in the propulsive nozzle of a solid propellant rocket motor requires five unit processes: interior, solid boundary, inlet boundary, centerline, and exit boundary points, as illustrated in Fig. 5. The unit processes for the interior and solid, inlet, and exit boundary points were based on the cylindrical coordinate forms of the governing equations. The Cartesian coordinate forms of the governing equations were employed for the centerline points (including the inlet centerline point), because the cylindrical coordinate forms of the governing equations are singular on the centerline.

A coordinate transformation was employed to transform the governing equations into an equally spaced finite difference grid. The following coordinate transformation was employed for the axisymmetric nozzle geometry:

$$\zeta=\arctan(z) \quad \text{and} \quad \eta=r/r_w(z) \quad (7)$$

where $r_w(z)$ is the physical wall radius. The arctangent function was employed for the axial transformation because it allows points to be packed more closely in the nozzle throat. Equation (7) was used to transform Eqs. (1-5) from (r,θ,z,t) physical space to (η,θ,ζ,t) computational space.

MacCormack's explicit finite difference method[8] was employed in all of the unit processes, except at the exit boundary points where Eaton and Zumwalt's[9] finite difference method was employed. The unit processes for the interior, centerline (except for the inlet centerline point), and exit boundary points employed the transformed governing equations directly. At inlet boundary points and solid boundary points, Kentzer's[10] method was employed to obtain the appropriate forms of the governing equations.

Centerline Points

The cylindrical coordinate forms of the governing equations, Eqs. (1-5), are singular on the centerline ($r=0$). Consequently, as suggested by Reyhner,[11] the Cartesian forms of the governing equations were employed to obtain the solution on the centerline. The Cartesian grid network at the centerline is illustrated in Fig. 6. The Cartesian forms of the governing equations were employed to obtain the solution at the centerline point itself, point 0, and at the interior points labeled 1-4. The solution at points 5-8 was obtained with the cylindrical coordinate forms of the governing equations. The flow properties at points 9-12, which are required in the solution for points 1-4, were obtained by quadratic bivariate interpolation. When the solution at points 0-8 has been obtained, quadratic bivariate interpolation is employed to determine the flow properties at the interior points with radial index $j=2$, which are required for the solution at interior points with radial index $j=3$.

Kentzer's Method

A form of the method of characteristics suggested by Kentzer[10] was employed to impose the solid and inlet boundary conditions. Ordinarily, an MOC solution involves construct-

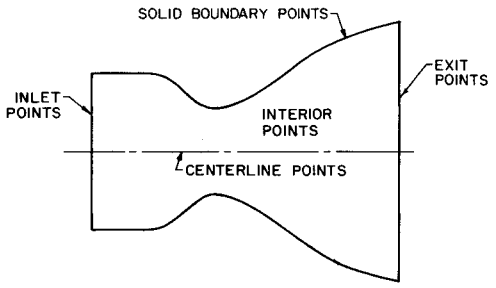

Fig. 5 Flowfield unit processes.

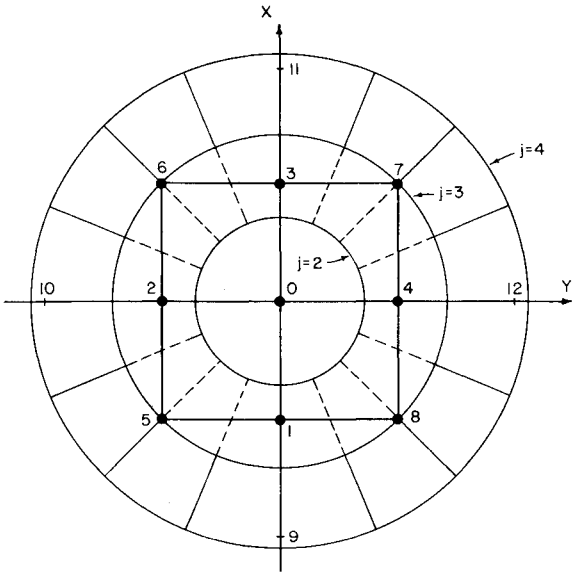

Fig. 6 Cartesian grid network at the centerline.

ing the finite difference grid in the characteristic hypersurfaces, and then applying the compatibility relations in the characteristic hypersurfaces. That approach is difficult to implement because of its complexity and is somewhat inefficient since it requires a considerable amount of flow property interpolation in the initial-value domain, which in three space dimensions is very time consuming. The MOC is, however, very accurate due to the close matching of the finite difference grid with the physics of the problem. Therefore, it is advantageous to use the MOC. Kentzer's method resolves this dilemma by applying the compatibility relations directly in the coordinate directions rather than in the characteristic hypersurfaces. This approach circumvents the complexity of a full MOC treatment, while retaining good accuracy (see Ref. 12).

At every point in a flowfield there are two infinite families of characteristic hypersurfaces: stream hypersurfaces whose envelope is the pathline, and wave hypersurfaces whose envelope is the Mach hyperconoid. Compatibility relations are linear combinations of the original governing equations, which are interior operators, or directional derivatives, within a hypersurface. On each stream hypersurface there are three independent compatibility relations and on each wave hypersurface there is one independent compatibility relation. Since there are two infinite families of characteristic hypersurfaces at every point in a flowfield, there are an infinite number of compatibility relations at every point. However, there are only five independent governing equations [i.e., Eqs. (1-5)]. Consequently, only five of the infinite number of compatibility relations are independent. Rusanov has shown that only three independent sets of compatibility relations exist for unsteady three-dimensional flow. The set employed in the present investigation consists of one compatibility relation applied along a pathline, two compatibility relations applied along any two independent stream hypersurfaces, and one compatibility relation applied along any two independent wave hypersurfaces. These results are presented in Refs. 1 and 2.

At boundary points, some of the characteristic hypersurfaces come from outside the flowfield and cannot be used. The boundary conditions are employed to replace the lost compatibility relations. Since the compatibility relations are merely linear combinations of all of the governing equations, all of the conditions that apply on the boundaries are included; namely, the governing equations and the boundary conditions. This procedure of combining the boundary conditions with the appropriate subset of the compatibility relations to obtain a unique set of equations which applies on the boundaries is the essence of Kentzer's method.[10]

The compatibility relations are written in terms of directional derivatives within a characteristic hypersurface. For stream hypersurfaces, the directional derivative takes the form

$$\frac{\mathrm{d}f}{\mathrm{d}t}=\frac{\partial f}{\partial t}+v_r\frac{\partial f}{\partial r}+\frac{v_\theta}{r}\frac{\partial f}{\partial \theta}+v_z\frac{\partial f}{\partial z} \tag{8}$$

and on the wave hypersurfaces,

$$\frac{\mathrm{d}f}{\mathrm{d}t}=\frac{\partial f}{\partial t}+(V_r-an_r)\frac{\partial f}{\partial r}+\frac{1}{r}(v_\theta-an_\theta)\frac{\partial f}{\partial \theta}$$

$$+(v_z-an_z)\frac{\partial f}{\partial z} \tag{9}$$

where n_r, n_θ, and n_z are the components in the r, θ, and z directions, respectively, of the unit normal to the wave hypersurface. In the numerical MOC, the characteristic hypersurfaces are constructed numerically, and the directional derivatives are evaluated as $\mathrm{d}f/\mathrm{d}t$ along each hypersurface. In Kentzer's method, the directional derivatives are evaluated in terms of the derivatives with respect to r, θ, z, and t, thus eliminating the necessity of constructing the characteristic hypersurfaces numerically. The terms in the directional derivatives are evaluated by the same finite difference method employed at the interior points.

Solid Boundary Points

At points on a solid wall, one wave hypersurface originates from outside of the flowfield. Thus, one boundary condition must be applied. That condition is that the velocity is parallel to the wall. Thus,

$$\bar{n}_b\cdot\bar{V}_{xyz}=0 \tag{10}$$

where $\bar{n}_b$ is the unit vector normal to the wall. Differentiating Eq. (10) with respect to time yields

$$\eta_{br}\frac{\partial v_r}{\partial t}+\eta_{b\theta}\frac{\partial v_\theta}{\partial t}+\eta_{bz}\frac{\partial v_z}{\partial t}=0 \tag{11}$$

where n_{br}, $n_{b\theta}$, and n_{bz} are the components of $\bar{n}_b$ in the r, θ, and z directions, respectively. The compatibility relations that apply at a solid boundary are given below. Those relations have been written with the time derivatives in the directional derivatives explicitly computed, and the space derivatives in the directional derivatives treated as source terms.

$$\frac{\partial p}{\partial t}-a^2\frac{\partial \rho}{\partial t}=\psi_1 \tag{12}$$

$$R_z\frac{\partial v_z}{\partial t}+R_r\frac{\partial v_r}{\partial t}+R_\theta\frac{\partial v_\theta}{\partial t}=\psi_2 \tag{13}$$

$$S_z \frac{\partial v_z}{\partial t} + S_r \frac{\partial v_r}{\partial t} + S_\theta \frac{\partial v_\theta}{\partial t} = \psi_3 \tag{14}$$

$$\frac{\partial p}{\partial t} - \rho a n_z \frac{\partial v_z}{\partial t} - \rho a n_r \frac{\partial v_r}{\partial t} - \rho a n_i \frac{\partial v_\theta}{\partial t} = \psi_4 \tag{15}$$

where R_r, R_θ, and R_z are the components of the unit vector which lies in the streamwise direction; S_r, S_θ, and S_z the components of the unit vector which lies in the stream hypersurface in a direction perpendicular to $\bar{R}$; n_r, n_i, and n_z the components of the unit vector normal to the wave hypersurface; and functions ψ_1-ψ_4 contain the space derivatives of v_r, v_θ, v_z, p, and ρ with respect to r, θ, and z.

Equations (11-15) are solved simultaneously to yield expressions for the time derivatives of v_r, v_θ, v_z, p, and ρ. A one-sided difference version of MacCormack's method is then applied to those equations to advance the solution in time. This procedure comprises the solid boundary point unit process.

Inlet Points

At inlet boundary points only one independent characteristic hypersurface originates from within the flowfield; thus, four boundary conditions must be applied. They are the known values of the stagnation pressure and temperature and two flow angles. The remaining condition is determined from the single compatibility relation that is valid along wave hypersurfaces. The following iterative procedure is employed. The Mach number M is assumed, p and T are calculated from the isentropic stagnation state relations, ρ is calculated from the equation of state, v_z from the wave hypersurface compatibility relation, v_r and v_θ from the specified flow angles, $\bar{V}$ from the velocity components, and a new value for M is calculated. The process is repeated to convergence. The wave hypersurface compatibility relation is solved by a one-sided version of MacCormack's method.

Exit Points

Exit boundary points are the points that lie at the downstream axial extent of the flowfield. These points may lie in the plane at the physical end of the nozzle or in the plane at the downstream extent of the region of interest in the nozzle (e.g., a plane slightly downstream from the nozzle throat where the flow is everywhere supersonic, that can be employed as the initial-value plane for an analysis of the downstream supersonic flowfield). The implementation of the exit, or outflow, boundary condition is very important. Eaton and Zumwalt[9] developed a method that treats the exit points as interior, centerline, or wall points, as appropriate, with one-sided (upwind) differencing for the axial derivatives. The other derivatives are treated as described in the preceding sections for the appropriate unit processes. Roache and Mueller[14] conducted comparative studies of several outflow (or exit) methods, with good results reported for Eaton and Zumwalt's method. Consequently, in the present study the exit points are calculated using Eaton and Zumwalt's method.

Code Verification

There are no known experimental data with which to compare the results of the present study. Verification of the computer code was accomplished by analyzing the case of nozzle rotation only and comparing with the results of the MOC analysis.

Numerical Results

Effects of Rotation

The nozzle geometry considered in this study is presented in Fig. 7. During flight, thrust vector control is obtained by rotating the supersonic portion of the nozzle relative to the missile to provide a thrust vector/nozzle axis misalignment. The nozzle center of rotation is located at the nozzle minimum area (geometric throat) plane. The missile center of rotation is located 92.37 in. upstream from the nozzle geometric throat plane. The motor operating conditions and gas properties are presented in Table 1.

The results presented in this section were obtained with the present three-dimensional time-dependent analysis in conjunction with the steady three-dimensional flow MOC program.[3] The present analysis is employed to analyze the flowfield in the subsonic/transonic portion of the nozzle rotating with the missile. This analysis provides a supersonic IVS from which the supersonic flowfield can be accurately determined by the MOC program. The entire subsonic/transonic/supersonic flowfield could be determined by the present analysis. However, for a quasisteady analysis such as considered here, it is much more efficient to compute the supersonic flowfield by the steady flow technique. For the purpose of this study, the nozzle rotation is segregated between the two analyses. The present analysis considers only missile rotation. It is assumed that only the diverging portion of the nozzle rotates relative to the missile, and that the nozzle rotation has a negligible effect on the portion of the transonic flowfield from the throat plane to the first fully supersonic plane downstream from the throat. The flowfield in this region is calculated by the present analysis, which does not consider nozzle rotation. Neither of these assumptions is limiting, however. The entire nozzle may actually rotate, depending on the location of the split line, but the converging portion is typically quite short relative to the diverging portion. Hence, the nozzle rotation moment arm is quite short and its effect relative to missile rotation should be small. The MOC analysis considers the effect of both missile and nozzle rotation. All results are for rotation in the pitch plane (i.e., about the y axis) only. The flow angles at the inlet to the subsonic nozzle were specified as zero.

Figure 8 presents the effects of missile and nozzle rotation on the torque acting on the supersonic portion of the nozzle. Figure 8 shows that the nozzle torque varies linearly with nozzle rotation rate for a fixed missile rotation rate. Missile rotation alone has a greater effect on the nozzle torque than nozzle rotation alone. The torque for a nonrotating missile with a nozzle rotation rate of 400 deg/s is -0.42×10^6 in.-lbf, whereas the torque for a missile rotating at 400 deg/s with a nonrotating nozzle is -1.38×10^6 in.-lbf, which is approximately 330% greater. This is to be expected, since the moment arm from the missile center of rotation is much larger than that from the nozzle center of rotation. Comparison of Figs. 8 and 2 reveals that for nozzle rotation only, the results of the present analysis and the previous study[3] are very similar. The effect of missile rotation is to cause a significant nozzle torque, even for a nonrotating nozzle, which varies linearly with nozzle rotation. The slopes of the curves for the different missile and nozzle rotation rates are approximately the same. Consequently, the nozzle torque for combined missile and nozzle rotation is approximately equal to the sum of the nozzle torques due to missile rotation alone and nozzle rotation alone.

Figure 9 presents the effect of rotation on the side force acting on the nozzle. The side force varies linearly with nozzle rotation rate for a given missile rotation rate. As with torque, the side force for missile rotation alone is higher than for nozzle rotation alone. A nonrotating missile with a nozzle rotation rate of 400 deg/s develops a -2500 lbf side force on the nozzle, while a missile rotating at 400 deg/s with a nonrotating nozzle develops a nozzle side force of -4900 lbf. Hence, the

Table 1 Data for the nozzle studies

Stagnation pressure, lbf/in.^{2}	4570
Stagnation temperature, °R	5987
Ratio of specific heats	1.15
Gas constant, (ft-lbf)/(lbm-°R)	57.85
Ambient pressure, lbf/in.^{2}	14.7
Misalignment angle, deg	0.0

effects of missile rotation on the subsonic/transonic flowfield have a significant effect on the side force and torque developed by the nozzle.

Figure 10 illustrates the effect of rotation on the wall pressure distribution at the supersonic IVS. These effects were obtained with the present analysis, which considers the effects of missile rotation only. The supersonic MOC program then used these values as the IVS with which to analyze the effects of missile and nozzle rotation on the supersonic flowfield. The supersonic IVS is located 3.2 in. from the throat plane. The radial dimension in Fig. 10 is the difference, or distortion, between the local wall pressure and the wall pressure at the nozzle circumferential position of 90 deg (which is identical to the wall pressure at 270 deg because the rotation is in the pitch plane only). The missile is rotated in an upward direction which results in an increase in the pressure on the bottom, or 180 deg position, of the nozzle wall and a decrease in the pressure on the top, or 0 deg position, of the nozzle wall. The wall pressure at 180 deg is increased by 10.3 psi to 1559.8 psia, and the wall pressure at 0 deg is reduced by 9.7 psi to 1539.8 psia. Increasing the missile rotation rate from 400 to 800 deg/s increases the distortion of the wall pressure profile as expected.

Figure 11 presents the wall pressure distortion at the nozzle exit plane (46.96 in. from the throat plane) for two nozzle rotation rates—200 and 400 deg/s—for a nonrotating missile. The radial dimension is the difference between the local wall pressure and the wall pressure at the nozzle circumferential position of 90 deg (which is identical to the wall pressure at 270 deg). The nozzle is rotated in an upward direction. The wall pressure at 90 deg is 167.6 psia and is essentially unaffected by rotation. Increasing the nozzle rotation rate from 200 to 400 deg/s increases the distortion of the wall pressure profile as expected. Also computed, but not shown in Fig. 11, was the pressure distortion resulting from a -400 deg/s nozzle rotation rate (i.e., downward nozzle motion). That computation resulted in the mirror image about the horizontal axis of the $\bar{\omega}_N = 400$ deg/s distortion curve, as it should.

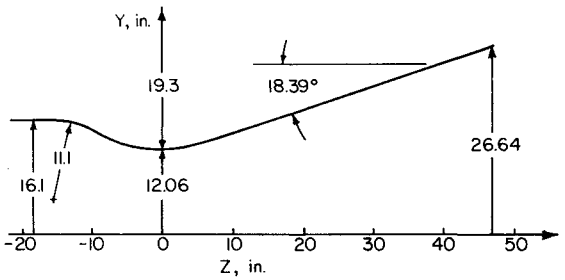

Fig. 7 Nozzle geometry.

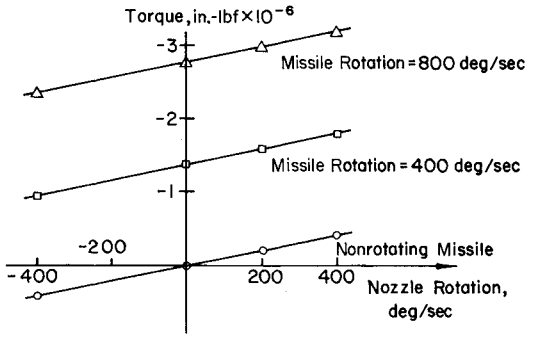

Fig. 8 Effect of rotation on torque.

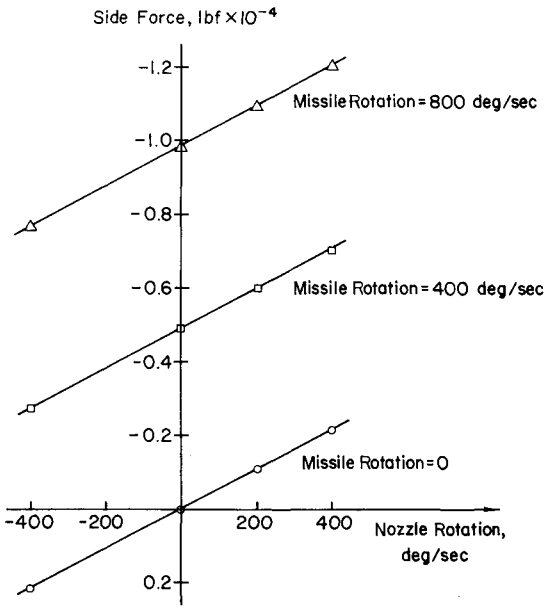

Fig. 9 Effect of rotation on side force.

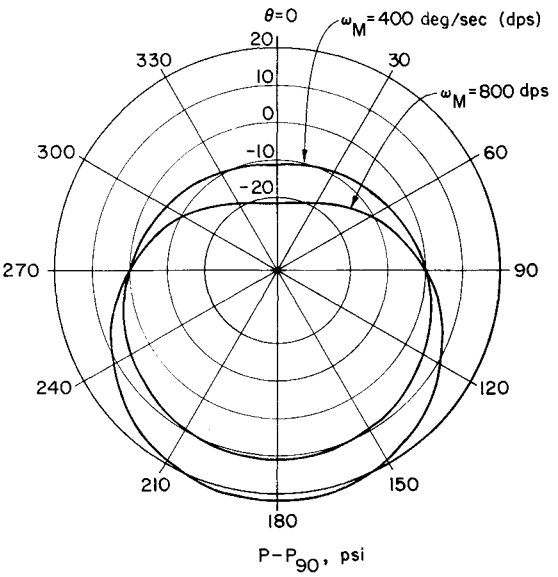

Fig. 10 Wall pressure distortion at the supersonic initial-value surface.

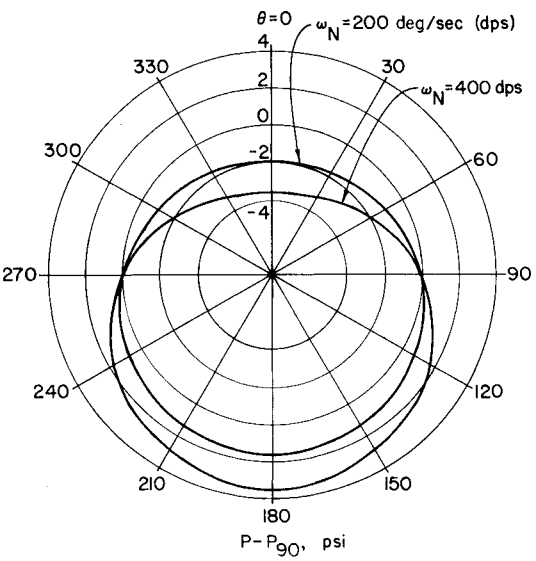

Fig. 11 Wall pressure distortion at the nozzle exit plane, nonrotating missile.

Figure 12 illustrates the exit plane wall pressure distortion for a missile rotation rate of 400 deg/s with nozzle rotation rates of 0, 200, 400, and −400 deg/s. The wall pressure at 90 and 270 deg is 168.8 psia and is essentially unaffected by nozzle rotation. Increasing the nozzle rotation rate to 200 and 400 deg/s increases the pressure distortion. A nozzle rotation rate of −400 deg/s results in effective cancellation of the pressure distortion.

Effects of Misalignment

The final study was concerned with assessing the effect of inlet flow misalignment on the flowfield. All of the studies discussed heretofore were concerned with the determination of the effects of missile and nozzle rotation on the flowfield in a nozzle for the special case of no misalignment between the axes of the nozzle and the rocket motor. Clearly, the general case would involve a misalignment between the nozzle and rocket motor axes to create a thrust vector misalignment. The effect of a nozzle inlet misalignment can be assessed by conducting a three-dimensional time-dependent analysis in which the nozzle inlet flow angle has been set equal to the misalignment angle between the nozzle and rocket motor axes. The results presented herein are for the two cases of 1- and 2-deg pitch-plane misalignment. This misalignment results in one plane of symmetry in the flowfield (the xz plane). Both cases consider nozzle inlet misalignment only (i.e., no missile or nozzle rotation).

To obtain the flowfield due to nozzle misalignment, the following procedure was employed. The time-dependent three-dimensional analysis developed in this study was first employed with the proper inlet flow angle to obtain the flowfield in the subsonic/transonic portion of the nozzle and a supersonic IVS just downstream from the nozzle throat. The three-dimensional MOC program[3] was then employed to continue the solution to the nozzle exit plane. The effect of nozzle misalignment alone is discussed in this section, but the combined effects of nozzle misalignment and missile and nozzle rotation could be analyzed with this procedure as well.

Figure 13 presents the ratio of side force to axial thrust as a function of nozzle length. For a nozzle misalignment of 2 deg, the calculated misalignment angle between the nozzle axis and the thrust vector is −0.222 deg at the nozzle inlet (16 in. upstream from the geometric throat plane). This value is the arctangent of the ratio of side force to axial thrust at the inlet plane. The sign of the misalignment angle indicates that the thrust vector angle at the IVS is (2.0 deg − 0.222 deg), or 1.778 deg. Thus, the flowfield does not achieve full turning and alignment with the nozzle in the entrance section. The thrust misalignment angle at the nozzle exit plane is 0.017 deg, which indicates that the net overall thrust vector angle is 2.017 deg with respect to the motor axis. Thus, the net effect of the underturned flow at the nozzle inlet plane is an overturned flow at the nozzle exit plane. Misalignments of the flowfield with respect to the nozzle may result in net thrust misalignments larger or smaller than and positive or negative with respect to the initial nozzle geometric misalignment. This phenomenon was observed previously by Hoffman and Maykut.[7]

Figure 14 presents the nozzle torque generated by nozzle misalignment. In addition to its effect on the missile turning

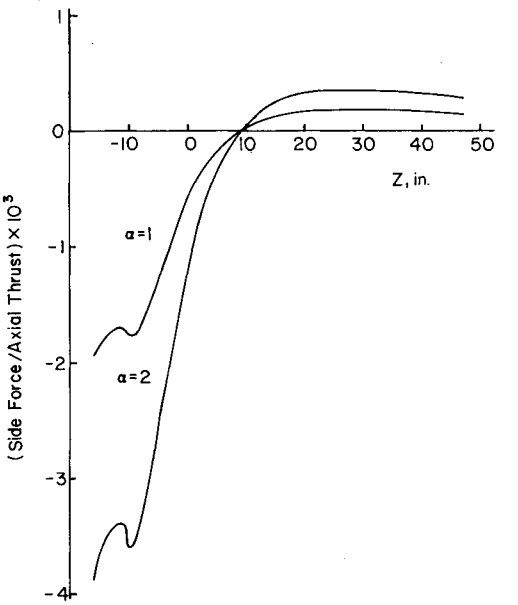

Fig. 13 Ratio of side force to axial force as a function of nozzle length.

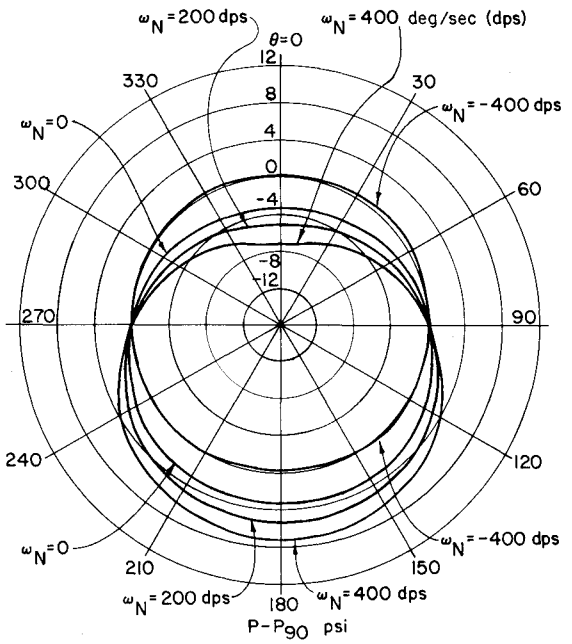

Fig. 12 Wall pressure distortion at the nozzle exit plane, rotating missile.

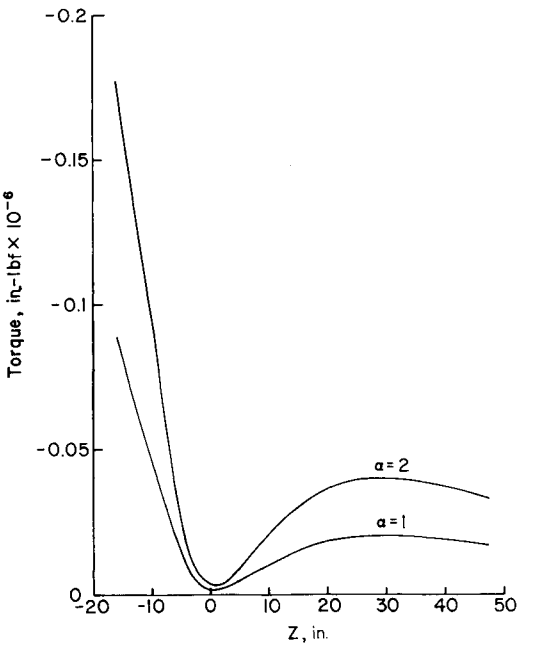

Fig. 14 Torque as a function of nozzle length.

torque, nozzle torque may be significant in the design of a movable nozzle actuation system. The net torque on the movable nozzle is the exit plane torque minus the initial-value plane torque. For 2-deg nozzle misalignment, the net nozzle torque is 0.144×10^6 in.-lbf. This torque is of the order of the torque calculated for this nozzle at a nozzle rotation rate of -120 deg/s for the case of a nonrotating missile, cf. Fig. 8. Clearly, the torque due to rotation may be as significant as the torque due to misalignment, and both must be considered in the design of a movable nozzle actuation system.

Conclusions

The governing equations for the unsteady three-dimensional inviscid flow of a gas through a rotating nozzle attached to a rotating missile have been derived. A numerical integration procedure and a computer program based on that procedure have been developed. The computer program determines the flowfield in the subsonic/transonic portions of the nozzle accounting for the effects of missile rotation, nozzle misalignment, or a combination of both. A supersonic initial-value surface downstream from the nozzle throat is generated, from which a steady three-dimensional method-of-characteristics analysis is used to continue the solution to the nozzle exit plane.

An analysis of the effects of missile and nozzle rotation on the flowfield was conducted, and the following conclusions were drawn. Nozzle torque varies linearly with nozzle rotation rate for fixed missile rotation rate. Missile rotation alone has a greater effect on nozzle torque than nozzle rotation alone. For combined missile and nozzle rotation, the resultant nozzle torque is approximately equal to the sum of the torque due to missile rotation alone and the torque due to nozzle rotation alone. The preceding conclusions apply to side forces as well. For misaligned inlet flow, the thrust vector angles may be larger or smaller than the corresponding geometric misalignment.

The present technique can be utilized to analyze the combined effect of missile and nozzle rotation on the flowfield, including angular acceleration, as well as the effects of nozzle misalignment.

Acknowledgments

This research was supported by the Ballistic Missile Defense Advanced Technology Center, Huntsville, Alabama, under Contract DASG60-75-C-0061 with Thiokol Corporation/Huntsville Division. Mr. R.H. Whiteside Jr. of Thiokol was the technical monitor of the Purdue program.

References

[1]Brown, J.J., "Unsteady Three-Dimensional Subsonic Flow in a Solid Propellant Rocket Motor Including the Effect of Motor Rotation," Ph.D. Thesis, Purdue University, West Lafayette, IN, Dec. 1979.

[2]Hoffman, J. D. and Brown, J. J., "Unsteady Three-Dimensional Subsonic Flow in a Solid Propellant Rocket Motor Including the Effect of Motor Rotation," Vols. I and II, Thiokol/Huntsville Division, Huntsville, AL, Rept. U-80-02, Dec. 1979.

[3]Hoffman, J. D. and Vadyak, J., "Analysis of the Effects of Rotation on the Thrust and Torque Developed by Propulsive Nozzles," Vols. I and II, Thiokol/Huntsville Division, Huntsville, AL, Rept. U-77-09, Oct. 1977.

[4]Cline, M. C., "VNAP: A Computer Program for Computation of Two-Dimensional, Time Dependent Compressible, Viscous, Internal Flow," Los Alamos Scientific Laboratory, Los Alamos, NM, Rept. LA-7326, Nov. 1978.

[5]Kliegel, J. R. and Levine, J. N., "Transonic Flow in Small Throat Radius of Curvature Nozzles," *AIAA Journal*, Vol. 7, July 1969, pp. 1375-1378.

[6]Vadyak, J., Hoffman, J. D., and Whitesides, R. H. Jr., "Analysis of the Effects of Rotation on the Forces and Moments Developed by Supersonic Propulsive Nozzles," *AIAA Journal*, Vol. 18, Jan. 1980, pp. 101-102.

[7]Hoffman, J. D. and Maykut, A. R., "Gas Dynamic Gain of Supersonic Thrust Nozzles," *Journal of Spacecraft and Rockets*, Vol. 11, Oct. 1974, pp. 697-704.

[8]MacCormack, R. W., "The Effect of Viscosity in Hypervelocity Impact Cratering," AIAA Paper 69-354, 1969.

[9]Eaton, R. R. and Zumwalt, G. W., "A Numerical Solution for the Flow Field of a Supersonic Cone-Cylinder Entering and Leaving a Blast Sphere Diametrically," Sandia Laboratories, Albuquerque, NM, Rept. SC-CR-67-2532, 1967.

[10]Kentzer, C. P., "Discretization of Boundary Conditions on Moving Discontinuities," *Proceedings of the Second International Conference on Numerical Methods in Fluid Dynamics*, Springer-Verlag, Berlin, 1970, pp. 108-113.

[11]Reyhner, T. A., "Transonic Potential Flow Around Axisymmetric Inlets and Bodies at Angle of Attack," *AIAA Journal*, Vol. 15, Sept. 1977, pp. 1299-1306.

[12]Abbett, M. J., "Computational Procedures for Inviscid, Supersonic Steady Flow Field Calculations," NASA-CR-14446, 1971.

[13]Rusanov, V. V., "The Characteristics of General Equations of Gas Dynamics," *Zhurnal Vychislitelnoi Matematiki i Mathematicheskoi Fiziki*, Vol. 3, 1963, pp. 508-527.

[14]Roache, P. J. and Mueller, T. J., "Numerical Solutions of Compressible and Incompressible Laminar Separated Flows," AIAA Paper 68-741, June 1968.